Operational Implementation of Sea Ice Concentration Estimates From the AMSR2 Sensor

Walter N. Meier, J. Scott Stewart, Yinghui Liu, Jeffrey Key, and Jeffrey A. Miller

***Abstract*—An operation implementation of a passive microwave sea ice concentration algorithm to support NOAA's operational mission is presented. The NASA team 2 algorithm, previously developed for the NASA advanced microwave scanning radiometer for the Earth observing system (AMSR-E) product suite, is adapted for operational use with the JAXA AMSR2 sensor through several enhancements. First, the algorithm is modified to process individual swaths and provide concentration from the most recent swaths instead of a 24-hour average. A latency (time since observation) field and a 24-hour concentration range (maximum–minimum) are included to provide indications of data timeliness and variability. Concentration from the Bootstrap algorithm is a secondary field to provide complementary sea ice information. A quality flag is implemented to provide information on interpolation, filtering, and other quality control steps. The AMSR2 concentration fields are compared with a different AMSR2 passive microwave product, and then validated via comparison with sea ice concentration from the Suomi visible and infrared imaging radiometer suite. This validation indicates the AMSR2 concentrations have a bias of 3.9% and an RMSE of 11.0% in the Arctic, and a bias of 4.45% and RMSE of 8.8% in the Antarctic. In most cases, the NOAA operational requirements for accuracy are met. However, in low-concentration regimes, such as during melt and near the ice edge, errors are higher because of the limitations of passive microwave sensors and the algorithm retrieval.**

***Index Terms*—AMSR2, Antarctic, Arctic, passive microwave, remote sensing, sea ice.**

I. Introduction

ARCTIC sea ice estimates from passive microwave sensors provide one of the longest and most complete remote sensing climate indicators. A series of multichannel satellite-borne passive microwave imagers have been providing a near-continuous daily time series since late 1978. The passive microwave retrievals do not rely on solar radiation and generally are minimally affected by the atmospheric emission, so these sensors provide near-complete coverage of sea ice covered regions.

Because of their continuous and near-complete coverage, passive microwave sea ice data have long been used as a climate indicator, as input and validation for climate models, and to assess environmental impacts on biology and the coast. Passive microwave sea ice fields have also been employed in operational ice analyses. However, their use has become more limited over time for two reasons. First, passive microwave imagery has been relatively low spatial resolution—25 km gridded, but the sensor footprints of some input channels were often lower, so the effective resolution could be as low as 40–70 km. Second, passive microwave data have limitations during melt and in the marginal ice zone where thin ice tends to be underestimated; both of these regions are of particular interest for operational ice mapping.

With the launch of RADARSAT in 1995, the availability of synthetic aperture radar (SAR) imagery became more widespread. The high-resolution (<500 m) all-sky capabilities largely superseded the use of passive microwave imagery by operational ice charting organizations [1]. However, for operational modeling, passive microwave sea ice data have remained useful because of their complete daily coverage. The resolution limitation is not as critical for models because the model resolution is no higher than the satellite data.

The advanced microwave scanning radiometer 2 (AMSR2) sensor provides a new resource for operational sea ice applications with its enhanced spatial resolution (5–10 km). AMSR2 was launched in 2012 on Japan's Global Change Observation Mission 1st - Water "SHIZUKU" (GCOM-W1) satellite. It is effectively a replacement for AMSR for the Earth observing system (AMSR-E), onboard NASA's Aqua satellite, which stopped regular scanning in October 2011. Here, we describe an implementation of an AMSR2-derived sea ice concentration algorithm for NOAA operational products. It is based off of well-validated heritage algorithms, but is optimized for operational processing and includes additional ancillary fields and quality flags.

II. NOAA Operational Requirements

NOAA is supporting the development and implementation of operational products derived from AMSR2. The goal of this

Manuscript received December 9, 2016; revised March 15, 2017; accepted March 21, 2017. Date of publication May 1, 2017; date of current version September 20, 2017. This work was supported in part by the National Oceanic and Atmospheric Administration Joint Polar Satellite System program and in part by NASA. *(Corresponding author: Walter N. Meier.)*

W. N. Meier is with the NASA Goddard Space Flight Center Cryospheric Science Lab, Greenbelt, MD 20771 USA (e-mail: walt.meier@nasa.gov).

J. S. Stewart is with the National Snow and Ice Data Center, Boulder, CO 80309 USA (e-mail: scottincolorado@gmail.com).

Y. Liu is with the Cooperative Institute for Meteorological Satellite Studies, University of Wisconsin, Madison, WI 53706 USA (e-mail: yinghuil@ssec.wisc.edu).

J. Key is with the NOAA National Environmental Satellite, Data, and Information Service, Madison, WI 53706 USA (e-mail: jeff.key@noaa.gov).

J. A. Miller is with the NASA Goddard Space Flight Center Cryospheric Science Lab, Greenbelt, MD 20771 USA, and also with ADNET Systems, Inc., Bethesda, MD 20817 USA (e-mail: Jeffrey.a.miller@nasa.gov).

Digital Object Identifier 10.1109/JSTARS.2017.2693120

TABLE I
JPSS REQUIREMENTS FOR THE NOAA GCOM-W1/AMSR2 SEA ICE CONCENTRATION PRODUCT

EDR Attribute	Threshold	Objective
Applicable conditions	Delivered under "all weather" conditions	Delivered under "all weather" conditions
Horizontal cell size	10 km	5 km
Mapping uncertainty, 3 sigma	5 km	3 km
SIC and MYIC Range	0–100%	0–100%
Ice age classes	Ice free, first-year, multiyear ice	Ice free, nilas, grey white, grey, white, first year medium, first year thick, second year, and multiyear; smooth and deformed ice
Measurement uncertainty, ice concentration	10%	5%
Probability of correct typing of ice age classes	70%	90%
Refresh	At least 90% coverage of the globe about every 20 h (monthly average)	Not Specified

NOAA effort is not to develop completely new algorithms, but rather to adapt or enhance existing algorithms for operational applications when possible. Several environmental variables that are key to NOAA's operational mission can be derived from passive microwave imagery. NOAA's AMSR2 products are being implemented for operational generation in two phases. The "day 1" products include calibrated brightness temperatures, total precipitable water, cloud liquid water, sea surface temperature, sea surface wind speed, and precipitation type and rate. The "day 2" products are snow cover, snow depth, snow water equivalent, sea ice characterization, soil moisture, and surface type. The sea ice characterization product, which is the subject of this paper, includes ice concentration and ice age/type.

NOAA has myriad operational objectives that require input sea ice fields. Weather models require sea ice as a boundary condition. Sea ice is critical for navigation and other activities in and near ice-infested waters. For these applications, the U.S. National Ice Center (NIC) produces weekly ice charts and daily ice edge products [1]. As noted above, NIC relies primarily on higher resolution imagery, such as from SAR or MODIS. But AMSR2's complete all-sky coverage is useful to fill in potential data gaps. The AMSR2 data also provide enhanced initialization fields over sea ice forecast models run by the U.S. Navy, which supports NIC analyses as well [2].

The NOAA–NASA joint polar satellite system (JPSS) specifies product performance requirements for spatial resolution, mapping uncertainty, measurement range, measurement uncertainty, coverage, and refresh rates. The requirements for the sea ice characterization product, or "environmental data record" (EDR), are presented in Table I [3]. The threshold requirements represent the baseline JPSS performance. It is expected, however, that efforts will continue toward improving products over the life of the JPSS program to the point where the more stringent objective requirements may be met. At present, only the threshold requirements must be met.

III. Algorithm Description

The primary sea ice concentration algorithm is the NASA team 2 (NT2) [4], an enhancement to the original NASA team [5] algorithm. The enhancements include the incorporation of the high-frequency (89 GHz) channels to reduce sensitivity to surface inhomogeneity. Because the high-frequency channels are more sensitive to atmospheric emission, a radiative transfer model is employed to correct the brightness temperature. The model is used to derive coefficients, called tie points, for three surface types—two ice and one water—for each of 12 atmospheres that represent typical polar conditions. These modeled pure surface type T_bs are then combined for each concentration combination in 1% intervals for all concentrations, 0–100% and used to calculate two T_b ratios. This effectively creates a $12 \times 101 \times 101$ look-up table (12 atmospheres, two ice types with possible concentrations of 0–100%).

The estimation of the observed concentration is iterative, where the modeled brightness temperatures for different atmospheric conditions are adjusted through the $12 \times 101 \times 101$ look-up table to minimize a cost function of the difference between the model and observed brightness temperatures. The sea ice concentration is the sum of the two sea ice type concentrations for which the cost function is a minimum. Unlike many passive microwave sea ice concentration algorithms that use daily gridded average T_bs for input, the NT2 algorithm should be run on swath T_b input because the effectiveness of the weather correction may be degraded by averaging T_bs over 24 h.

There are also postprocessing steps to remove erroneous data. First, two gradient ratio weather filter thresholds are used, one for 36 and 18 GHz, and one for 23 and 18 GHz. These remove false ice over the open ocean that can occur due to strong atmospheric emission (e.g., precipitation) or wind roughening of the ocean that raises the surface emission. A land-spillover correction is applied near the coast to remove spurious ice that can occur because the algorithm interprets mixed land–ocean cells as sea ice. Finally, a monthly ocean SST climatology mask is applied to remove any remaining ice in regions where sea ice is not possible because the oceans are too warm.

The NT2 algorithm is used to produce the NASA AMSR-E standard sea ice concentration products [6] and is described in further detail in [7]. It has been chosen as the NOAA operational algorithm because of its long heritage and thorough validation (e.g., [8]). The basic algorithm is unchanged, but it has been modified for the operational implementation, as outlined in the next section.

IV. Operational Implementation

Several modifications, some relatively minor, some more substantial, have been made to the basic algorithm to better facilitate operational use. The grid, processing method, and output parameters are described below. The output parameters and valid values in the product are provided in Table II.

A. Intercalibration With AMSR-E

The NT2 algorithm was originally developed for the AMSR-E and the derived coefficients [7] are sensor specific. To apply

TABLE II
OUTPUT STRUCTURE AND PARAMETERS OF SEA ICE PRODUCT

EDR Output	Description	Dynamic Range
NT2 SIC	Primary sea ice concentration estimate	0–100%
BT SIC	Secondary sea ice concentration estimate (no QC)	0–100%
NT2-BT SIC	Difference between NT2 and BT concentrations	–100 to +100%
SIC Range	Range of NT2 concentration over 24 h (max-min concentration)	0–100%
Age of observation	Age of observation on which concentration is based	0–1440 min
MYIC	Multiyear sea ice concentration (provisional)	0–100%
Quality Flag Field	Bitwise combination of quality conditions:	[4, 8, 16, 32, 64, 128]
	4: SST limited (SST mask applied)	
	8: Weather limited (weather filter threshold exceeded)	
	16: Land-spillover corrected (coastal ice removed)	
	32: Spatially interpolated (missing grid cells bi-linearly interpolated)	
	64: Missing (no valid T_b s found) 128: Land	

the algorithm for AMSR2 data, the AMSR2 T_bs are adjusted based on linear regression of T_bs with AMSR-E, as described in a companion paper in this special issue [9]. Effectively, the AMSR2 T_bs are adjusted to "equivalent-AMSR-E" T_bs so that the NT2 algorithm can be used as-is, without needing to rederive new coefficients and look-up tables.

B. EASE2 10 km Grid

The NT2 algorithm is run on swath data, but for convenience the output is typically gridded. Historically, a polar stereographic grid has been used for sea ice products, including the AMSR-E standard sea ice products [6]. However, a polar stereographic grid is nonstandard for many applications and using the sea ice data requires a regridding procedure, where information can be altered or lost. Here, we employ an equal area grid, EASE2 [10]–[12], which is an emerging standard for many polar applications. The fact that it is equal area simplifies calculations (e.g., total extent/area) and the underlying projection parameters (e.g., ellipsoid) are compatible with GIS and other modern image and data processing products. The EASE2 grid is a hemispheric projection. For the sea ice product, we have created a pair of subgrids (Northern and Southern Hemispheres) that covers all significant regions that may experience sea ice; for additional flexibility, the Northern Hemisphere grid also includes major lakes where ice can occur (Great Lakes, Caspian Sea, Black Sea). The result is a 10 km grid for both the Northern Hemisphere (1050 × 1050) and Southern Hemisphere (840 × 840) (see Fig. 1).

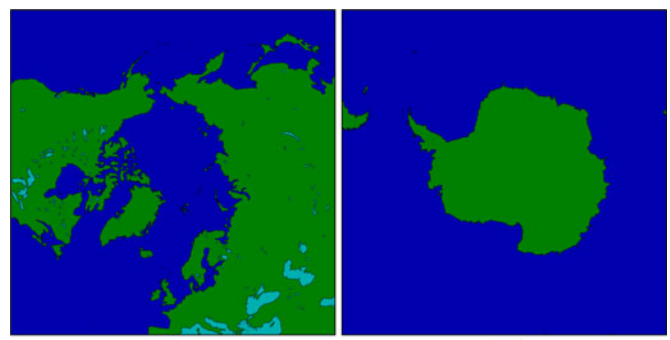

(a) (b)

Fig. 1. Map of coverage of EASE2 10 km grid for (a) Northern and (b) Southern Hemisphere. Ocean regions are in dark blue, lakes are in teal, and nonwater (land, ice sheet, ice shelf) regions are in green. Note that the Southern Hemisphere grid is smaller (840 × 840) than the Northern Hemisphere (1050 × 1050) but is scaled here to the same size image.

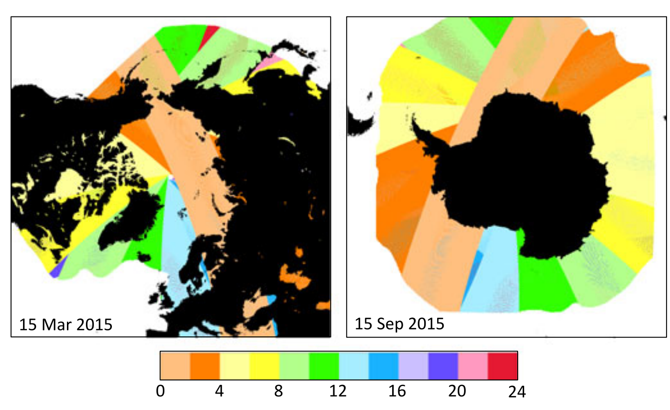

Fig. 2. Example data latency field for (a) the Northern Hemisphere on 15 March 2015 and (b) the Southern Hemisphere on 15 September 2015. These dates correspond to near the maximum extent for each hemisphere when the largest potential latency occurs. Each color represents a 2-hour interval of the time since 0Z of the given day. Note that the latency is only calculated within the "possible ice" region within the ocean mask.

C. Swath Updating and Latency Field

The original implementation of the NT2, while run on swath T_bs, is a once-daily gridded product averaging the concentrations from all swaths in a given day. Because there is considerable overlapping of swaths in the polar regions, some grid cells may have up to 6 swaths contributing to the daily concentration estimate at that location, while other grid cell concentrations will be from only 1 or 2 swaths.

In the NOAA implementation, a 24-hour period is maintained to provide complete fields, but the code has been modified to be updatable with each new swath and each grid cell contains only the most recent observation. There is no averaging of footprints from multiple swaths. When a new swath is processed, the concentrations derived from that swath replace previous observations. So the algorithm can be run as each new swath is acquired and the output field can be updated.

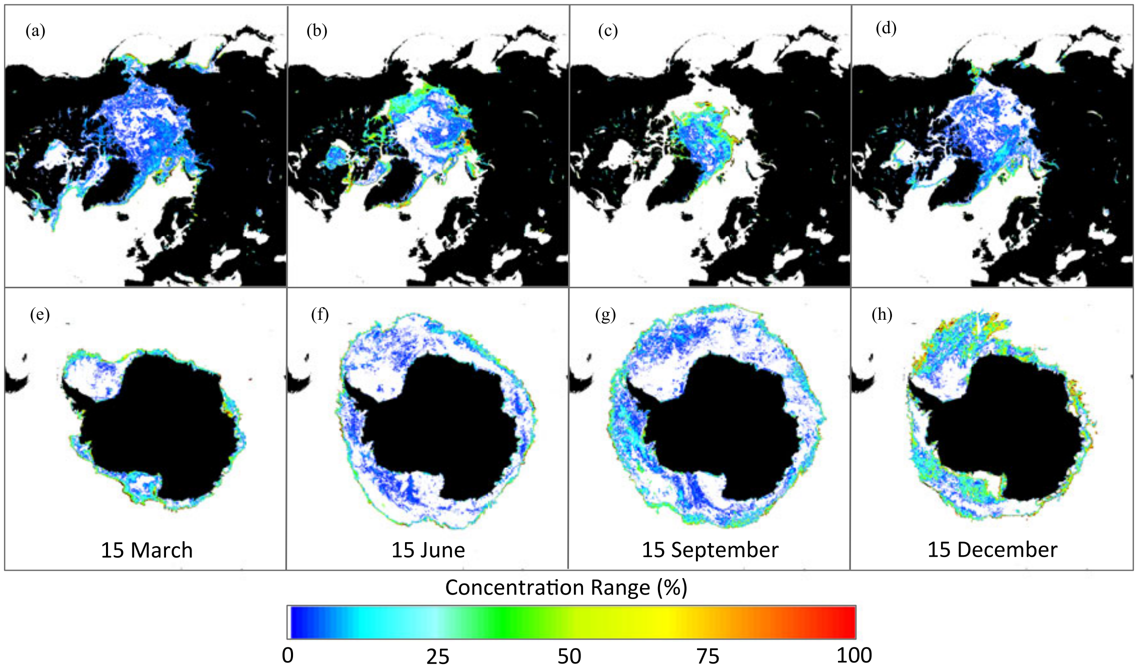

Fig. 3. Daily concentration range (maximum–minimum concentration) in 2015 for the Northern Hemisphere on (a) March 15, (b) June15, (c) September 15, (d) December 15, and (e-h) for the same dates in the Southern Hemisphere.

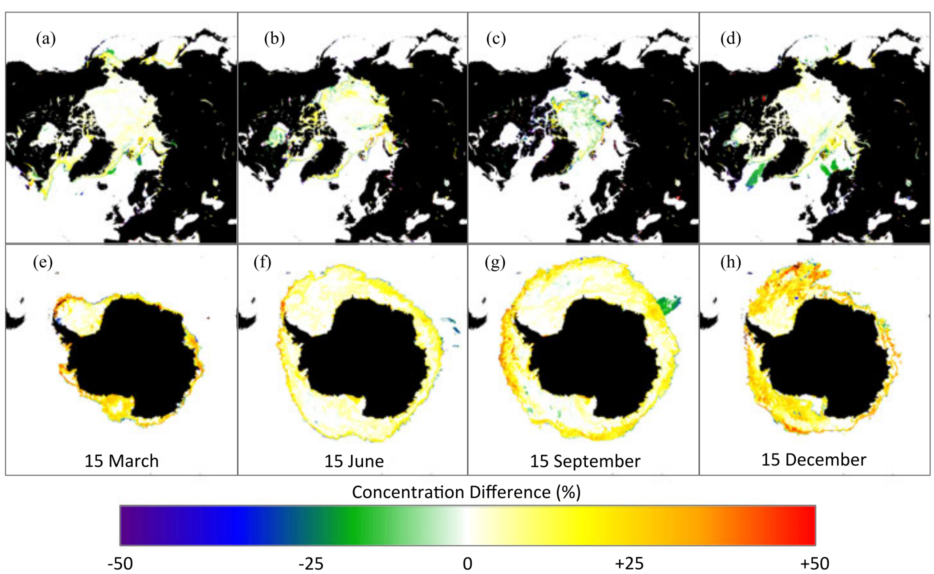

Fig. 4. NT2 minus Bootstrap concentration difference in 2015for the Northern Hemisphere on (a) March 15, (b) June15, (c) September 15, (d) December 15, and (e-h) for the same dates in the Southern Hemisphere.

A latency field (see Fig. 2) is included with the product that provides a time since observation. This allows users to know how old an observation is, update models with more recent data and/or temporally weight the estimates depending on the age of the estimate.

D. Daily Concentration Range

While each grid cell contains only the most recent observation, a daily concentration range field is produced. It contains the difference between the maximum and minimum concentration values obtained in the last 24 h in a given cell. This parameter provides an indication of how stable the concentration estimate has been through time. Where the max-min value is small, there has been little variation, which suggests that there has been little change in the sea ice state and that the algorithm is stable in the location. Where the max-min value is large, the sea ice has either been rapidly changing (growth/melt or significant ice advection) or the algorithm is less stable (perhaps due to changing atmospheric conditions). Thus, this daily variability parameter provides an indication of how much the sea ice has changed during the 24-hour period, either due to physical changes in the ice cover or due to algorithm variability.

Examples of the range field during different seasons (see Fig. 3) show that the region of large ranges is most typically at the ice edge. This is expected since the ice edge can vary substantially over 24 h due to ice growth, ice melt, and ice advection. At certain times of year, other regions also show higher ranges, most notably the Beaufort and Chukchi seas, north of Alaska on 15 June. This is due to surface melt and melt pond formation that tend to decrease the retrieved concentration and increase variability in the surface emission depending on surface and atmospheric conditions.

E. Bootstrap Algorithm Concentration

In addition to the NT2 algorithm, the Bootstrap algorithm is run as an ancillary concentration field. The Bootstrap algorithm has long heritage [13], has been widely used in the community, and is also a secondary field in the AMSR-E standard product. We include it in the operational product, along with the NT2 minus BT concentration difference field (see Fig. 4) to provide another estimate for comparison with NT2. When Bootstrap and NT2 yield substantially different concentration values, it suggests a higher uncertainty in the retrievals. The Bootstrap algorithm output does not include the postprocessing, so comparing it with NT2 also indicates where the postprocessing removed sea ice, allowing users to see the effect of the quality-control procedures and to potentially decide that ice may have been removed in error. This is most clearly seen in the Northern Hemisphere on 15 December [see Fig. 4(d)] and in the Southern Hemisphere on 15 September [see Fig. 4(g)] where clear weather artifacts are seen near the ice edge. These artifacts are likely due to wind roughening of the ocean surface or atmospheric effects such as water vapor, cloud liquid water, or rain [14].

F. Quality Flag Field

A final field consists of several flag values, combined in a bitwise manner to indicate quality control actions taken at a given cell (spatial interpolation, weather filter removal, land-spillover removal). Scattered grid cells with no data are filled with a simple spatial bilinear interpolation. Larger missing regions are left empty. Both of these conditions are also flagged in the quality field. The values for each condition are provided in Table II.

V. Validation

The NT2 algorithm has been well validated as part of the AMSR-E product validation efforts [8] as well via algorithm intercomparisons (e.g., [15]–[17]) and comparisons with operational estimates [18]. Here, we further assess the algorithm in its NOAA operational implementation. First, we compare total ice extent with the JAXA AMSR2 standard product (see Fig. 5). The JAXA product uses the Bootstrap algorithm, so the observed offset in extent values between the two algorithms is expected. The NT2 estimates are generally higher in winter, reflecting perhaps different sensitivities to thin ice and heavy snow cover [8]. In addition, ancillary influences such as coastal and weather effects may contribute to the differences. Despite the differences, the comparison shows that the NOAA product captures the seasonal cycle and synoptic variability, and yields estimates that are generally in agreement with another current AMSR2 sea ice product.

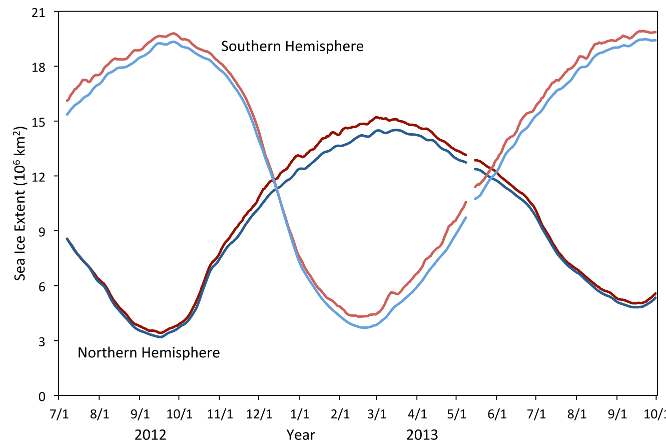

Fig. 5. Time series of NOAA NT2 (red shaded lines) and JAXA Bootstrap (blue shaded lines) total sea ice extent from AMSR2 for 3 July 2012 to 30 September 2013 for Northern Hemisphere and Southern Hemisphere (10–14 May are missing due to lack of sensor data). JAXA Bootstrap extent values obtained from the Arctic data archive system (ADS), which was developed by the National Institute of Polar Research (NIPR), https://ads.nipr.ac.jp/vishop/#/extent.

Second, we compare the AMSR2 ice concentration with sea ice concentrations from the Suomi visible and infrared imaging radiometer suite (VIIRS) instrument. The VIIRS ice concentration algorithm is described in detail in [19]. Briefly, the ice concentration, or the fraction of ice in any given pixel (C_p), is calculated as a linear combination of ice and water:

$$C_p = \frac{(B_p - B_{\mathrm{water}})}{(B_{\mathrm{ice}} - B_{\mathrm{water}})} \tag{1}$$

where B_{water} is the visible reflectance (daytime) or temperature (nighttime) of pure water, B_{ice} is the reflectance or temperature of pure ice, and B_p is the observed reflectance or temperature of the pixel. The VIIRS ice concentration is calculated in three steps. In the first step, clear VIIRS pixels are classified as ice or no-ice using a threshold method. In the second step, a tie-point algorithm is applied to determine the 0.64 μm reflectances or surface temperatures of pure ice in a search window. The pure water tie point is parameterized as function of solar zenith angle for reflectance, and as a function of salinity for surface temperature. The pure ice tie point is determined from the histogram of reflectances/temperatures in each search window. In the third step, ice concentration is calculated using (1). The original spatial resolution of the VIIRS ice concentration is 750 m. VIIRS ice concentration daily composites are then produced by remapping individual overpasses of VIIRS ice concentration to a 1 km EASE grid with newer cloud free data replacing older cloud free data.

For this validation study, sea ice concentration daily composites from VIIRS and AMSR2 from January 2016 to October 2016 were collocated and remapped to the 10 km EASE2-Grid.

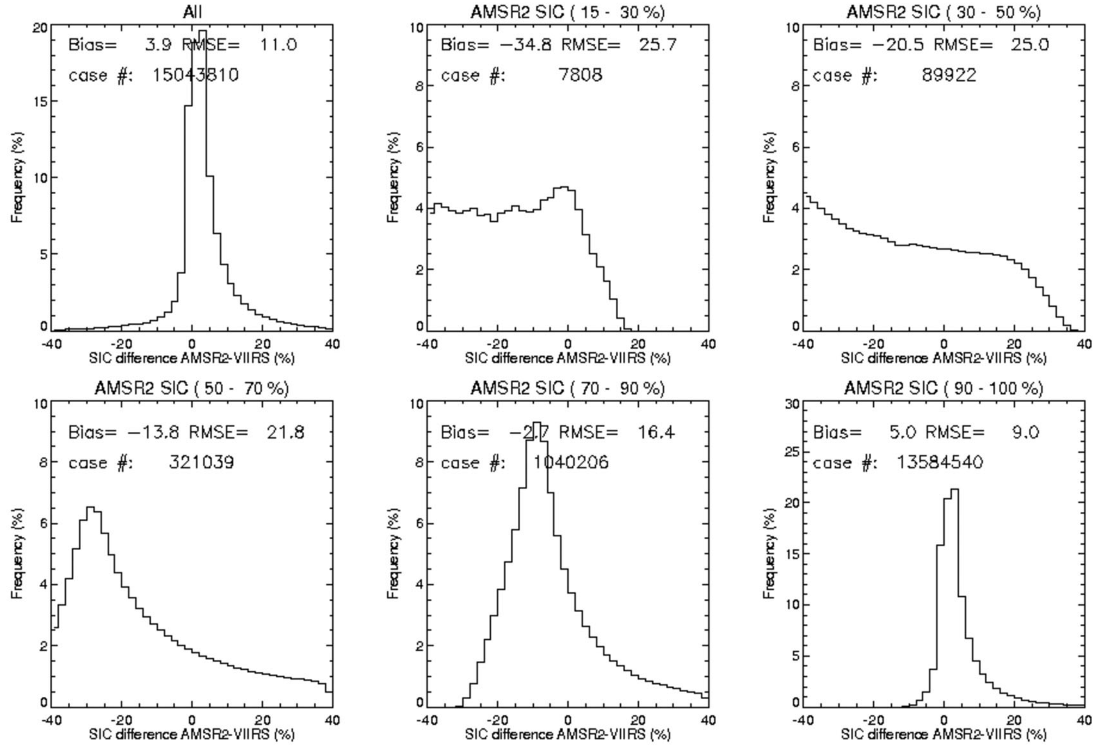

Fig. 6. Comparison of AMSR2 minus VIIRS ice concentrations for different AMSR2 ice concentration ranges/bins in the Arctic. The AMSR2 concentration is computed with the NASA team 2 algorithm. Note that the *y*-axis range is different for "All," "90–100%," and the other plots.

VIIRS ice concentration is calculated as the average of all 1 km EASE2 grid ice concentrations within a 10 km grid cell when more than 90% of those ice concentrations are available. It should be noted that the different spatial resolution of these two products, different instrument sensitivities (optical versus passive microwave), instrument field-of-view, and fundamental differences in the retrieval algorithms may all contribute to the difference of their comparisons.

Statistics employed in the validation are the bias and the root-mean-square error (RMSE). The bias is defined as the average difference between pixels in the two products. The RMSE is the square root of the mean squared difference between the two products. RMSE is also calculated with the bias removed, which is the square root of the average squared deviation of the errors from the mean error, or the standard deviation of the errors. For some applications, the absolute values of the bias, the RMSE, and the RMSE with the bias removed are termed as measurement accuracy, measurement uncertainty, and measurement precision, respectively.

Histograms of the differences between VIIRS and AMSR2 ice concentration match-ups for all cases and for AMSR2 concentration bins of 15–30%, 30–50%, 50–70%, 70–90%, and 90–100% are shown in Figs. 6 and 7 for cases in the Arctic and Antarctic. Only cases (pixels) with ice concentrations higher than 15% from both products are included. There are over 15 million and 17 million matched pairs for Arctic and Antarctic, respectively.

Over all ice concentration bins, the AMSR2 ice concentration biases are 3.9% for the Arctic (see Fig. 6) and 4.4% for the Antarctic (see Fig. 7). The corresponding RMSE values (with the bias not removed) are 11.0% and 8.8% for the Arctic and Antarctic, with majority of the ice concentration absolute differences less than 10.0%.

However, uncertainties within each AMSR2 ice concentration bin vary considerably. For the 90–100% AMSR2 ice concentration bins, the biases are positive and small for both Arctic and Antarctic. The differences become negative and larger for smaller AMSR2 ice concentrations, indicating that the AMSR2 ice concentration is significantly lower than the VIIRS ice concentration. This is not surprising. Low concentration indicates newly forming ice, melting ice, or simply very sparse ice cover—all conditions where passive microwave retrievals are less effective. Such conditions are also often typified by rapidly changing ice conditions, so the higher uncertainties may reflect changing ice conditions. Comparing contemporaneous imagery (e.g., individual swaths) could reduce some of these errors. Note that these low-concentration conditions occur in relatively few cases. The majority of comparisons occur in the 80–100% regime where the NT2 algorithm performs best. The low-concentration conditions are generally a small region of the sea ice cover, typically within $\sim$50 km of the ice edge. The RMSE with bias removed values (not shown) also increases with smaller AMSR2 ice concentrations.

The AMSR2-VIIRS comparison was also done for AMSR2 ice concentration calculated with the NASA Bootstrap algorithm. The results are very similar (not shown), with Arctic and Antarctic overall biases of 3.2% and –0.8%, and RMSE values of 11% and 10.8%. As with the NT2 algorithm, the biases increase significantly for lower AMSR2 ice concentration bins.

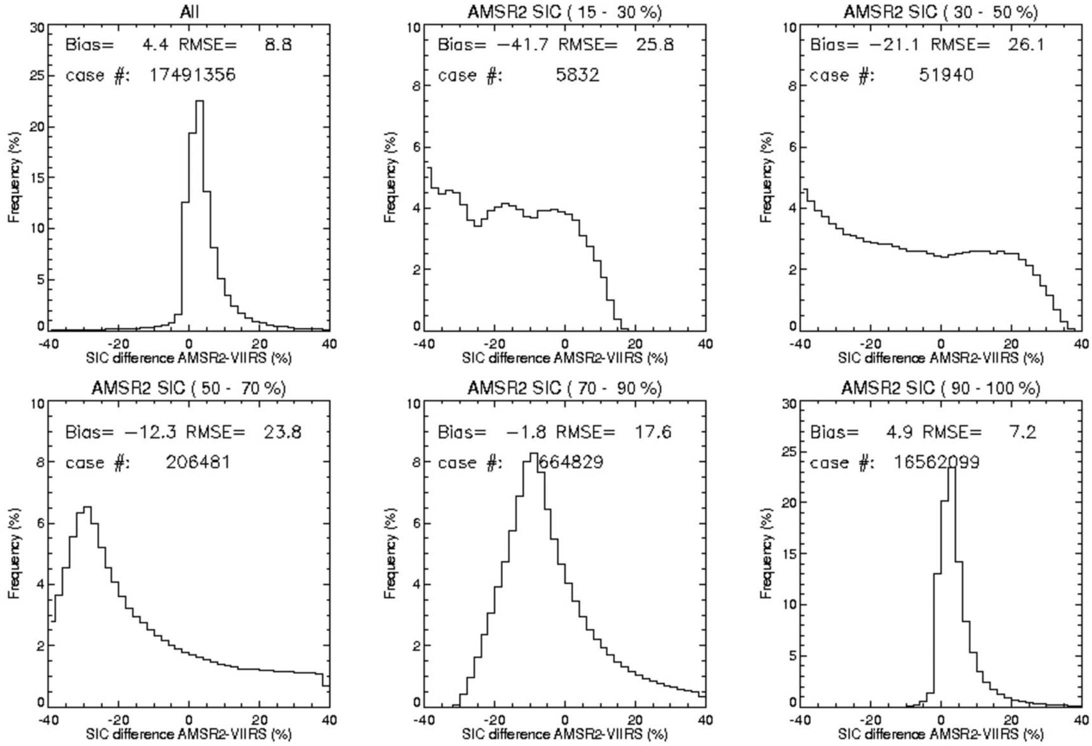

Fig. 7. Same as Figure 6 except for the Antarctic.

TABLE III
ACCURACY AND PRECISION OF AMSR2 COMPARED TO VIIRS CONCENTRATIONS FOR SEVERAL DATES IN 2015

	Northern Hemisphere			Southern Hemisphere		
Date	Accuracy	Precision	Samples	Accuracy	Precision	Samples
01/30	1.61	8.76	123 747	0.50	21.45	22 776
01/31	1.62	9.10	124 514	1.53	22.03	19 556
02/27	2.05	9.91	122 376	1.04	20.19	20 101
02/28	2.03	9.35	120 343	0.21	20.88	22 256
03/30	2.45	10.01	122 108	1.52	14.90	48 343
03/31	2.12	9.39	118 841	2.48	15.24	43 737
04/30	3.02	11.98	88 959	1.85	12.64	79 228
04/31	3.01	11.87	79 756	2.24	12.62	82 094
05/30	3.20	11.46	65 418	2.19	13.03	99 093
05/31	3.22	11.92	70 990	1.80	12.97	104 142
06/30	2.19	14.05	56 864	1.55	11.08	121 964
06/31	1.89	14.41	55 580	1.56	11.78	123 805
07/30	1.89	18.33	35 577	2.43	12.62	142 350
07/31	2.53	18.20	38 069	2.58	12.34	138 524
08/30	0.25	18.48	28 727	2.79	11.87	133 027
08/31	0.61	17.19	27 315	2.95	12.71	142 208

Histograms were produced for several days through 2015 under varying ice conditions. As expected, the performance of the algorithm is best under winter conditions, with larger errors during the summer melt season (see Table III).

VI. CONCLUSION

This paper presents a new operational implementation of the NT2 sea ice concentration algorithm for NOAA's AMSR2 product suite. The algorithm has been modified to be processed with each new incoming swath and each cell has only a single time-stamped observation instead of a daily average of all sensor observations. Additional ancillary fields are also added to address potential operational needs. These include: a latency field indicating the time since a given observation was obtained, a daily concentration variation (maximum–minimum concentration over past 24 h), a difference field with Bootstrap algorithm output, and a quality flag field with indications of quality control filtering.

Validation of the product indicates a good consistency with other AMSR2 sea ice products and overall good agreement with concentrations derived from VIIRS visible and infrared imagery. Overall, the performance meets the NOAA requirement of 10% uncertainty, but in low-concentration regimes errors can be higher. Future work will attempt to characterize and improve performance in these low-concentration regions. The product is currently pre-operational and data will soon be available via the operational GCOM-W1 AMSR2 products system from the NOAA NESDIS Office of Satellite and Product Operations (http://www.ospo.noaa.gov/Products/atmosphere/gpds/).

Sea ice concentration and extent from passive microwave instruments constitute one of the longest satellite-derived climate records and are one of the most iconic indicators of climate change. The AMSR2 sensor is carrying on the passive microwave record. As of May 2017, AMSR2 will have reached its nominal 5-year mission. It will continue to be supported as long as the sensor is functional. However, the other operating legacy sensors (DMSP SSMIS) used for sea ice are even older than AMSR2. New sensors have been proposed or approved, but it is likely to be at least 2022 before the next new passive microwave sensor is launched. Thus, there is an increasing risk of a gap in coverage as AMSR2 ages.

Acknowledgment

The views, opinions, and findings contained in this report are those of the author(s) and should not be construed as an official National Oceanic and Atmospheric Administration or U.S. Government position, policy, or decision.

References

[1] K. R. Dedrick, K. Partington, M. Van Woert, C. A. Bertoia, and D. Benner, "U.S. National/Naval Ice Center digital sea ice data and climatology," *Can. J. Remote Sens.*, vol. 27, no. 5, pp. 457–475, 2001. Doi: 10.1080/07038992.2001.10854887.

[2] P. G. Posey *et al.*, "Improving Arctic sea ice edge forecasts by assimilating high horizontal resolution sea ice concentration data into the US Navy's ice forecast systems," *Cryosphere*, vol. 9, pp. 1735–1745, 2015. Doi: 10.5194/tc-9-1735-2015.

[3] NOAA, "Joint polar satellite system level 1 requirements supplement, version 2.10," National Oceanic and Atmospheric Administration, Washington, DC, USA, 2014, 138 pp. [Online]. Available: http://www.jpss.noaa.gov/assets/pdfs/technical_documents/level_1_requirements_supplement.pdf

[4] T. Markus and D. J. Cavalieri, "An enhancement of the NASA Team sea ice algorithm," *IEEE Trans. Geosci. Remote Sens.*, vol. 38, no. 3, pp. 1387–1398, May 2000.

[5] D. J. Cavalieri, P. Gloersen, and W. J. Campbell, "Determination of sea ice parameters with the Nimbus-7 scanning multichannel microwave radiometer," *J. Geophys. Res.*, vol. 89, pp. 5355–5369, 1984.

[6] D. J. Cavalieri, T. Markus, and J. C. Comiso, "AMSR-E/aqua daily L3 12.5 km brightness temperature, sea ice concentration, & snow depth polar grids, version 3," NASA National Snow and Ice Data Center Distributed Active Archive Center, Boulder, CO, USA, 2014. Doi: http://dx.doi.org/10.5067/AMSR-E/AE_SI12.003.

[7] T. Markus and D. J. Cavalieri, "The AMSR-E NT2 sea ice concentration algorithm: It's basis and implementation," *J. Remote Sens. Jpn.*, vol. 29, no. 1, pp. 216–225, 2009.

[8] D. J. Cavalieri, T. Markus, D. K. Hall, A. J. Gasiewski, M. Klein, and A. Ivanoff, "Assessment of EOS Aqua AMSR-E Arctic sea ice concentrations using Landsat-7 and airborne microwave imagery," *IEEE Trans. Geosci. Remote Sens.*, vol. 44, no. 11, pp. 3057–3069, Nov. 2006. Doi: 10.1109/TGRS.2006.878445.

[9] W. N. Meier and A. Ivanov, "Intercalibration of AMSR2 NASA Team 2 algorithm sea ice concentrations with AMSR-E slow rotation data," *IEEE J. Sel. Topics Appl. Earth Observ. Remote Sens.*, 2017, to be published.

[10] M. J. Brodzik and K. Knowles, "EASE-grid 2.0 land-ocean-coastline-ice masks derived from Boston University MODIS/terra land cover data," NASA National Snow and Ice Data Center Distributed Active Archive Center, Boulder, CO, USA, 2011. Doi: http://dx.doi:10.5067/VY2JQZL9J8AQ.

[11] M. J. Brodzik, B. Billingsley, T. Haran, B. Raup, and M. H. Savoie, "EASE-Grid 2.0: Incremental but significant improvements for earth-gridded data sets," *ISPRS Int. J. Geo-Inf.*, vol. 1, no. 1, pp. 32–45, 2012. Doi: 10.3390/ijgi1010032.

[12] M. J. Brodzik, B. Billingsley, T. Haran, B. Raup, and M. H. Savoie, "Correction: Brodzik, M. J. *et al.* EASE-Grid2.0: Incremental but significant improvements for earth-gridded data sets, ISPRS Int. J. Geo-Information 2012, vol. 1, pp. 32–45," *ISPRS Int. J. Geo-Inf.*, vol. 3, no. 3, pp. 1154–1156, 2014. Doi: 10.3390/ijgi3031154.

[13] J. C. Comiso, "Enhanced sea ice concentrations and ice extents from AMSR-E Data," *J. Remote Sens. Jpn.*, vol. 29, no. 1, pp. 199–215, 2009.

[14] S. Andersen, R. Tonboe, S. Kern, and H. Schyberg, "Imrpoved retrieval of sea ice total concentration from spaceborne passive microwave observations using numerical weather prediction model fields: An intercomparisons of nine algorithms," *Remote Sens. Environ.*, vol. 104, pp. 374–392, 2006. Doi: L10.1016/j.rse.2006.05.013.

[15] N. Ivanova, O. M. Johannessen, L. T. Pedersen, and R. T. Tonboe, "Retrieval of Arctic sea ice parameters by satellite passive microwave sensors: A comparison of eleven sea ice concentration algorithms," *IEEE Trans. Geosci. Remote Sens.*, vol. 52, no. 11, pp. 7233–7246, Nov. 2014. Doi: 10.1109/TGRS.2014.2310136.

[16] S. Andersen, R. T. Tonboe, L. Kaleschke, G. Heygster, and L. T. Pedersen, "Intercomparison of passive microwave sea ice concentration retrievals over the high-concentration Arctic sea ice," *J. Geophys. Res.*, vol. 112, no. C8, pp. C08004-1–C08004-18, 2007.

[17] W. N. Meier, "Comparison of passive microwave ice concentration algorithm retrievals with AVHRR imagery in the Arctic peripheral seas," *IEEE Trans. Geosci. Remote Sens.*, vol. 43, no. 6, pp. 1324–1337, Jun. 2005.

[18] W. N. Meier, F. Fetterer, J. S. Stewart, and S. Helfrich, "How do sea ice concentrations from operational data compare with passive microwave estimates? Implications for improved model evaluations and forecasting," *Ann. Glaciol.*, vol. 56, no. 69, pp. 332–340, 2015. Doi: 10.3189/2015AoG69A694.

[19] Y. Liu, J. Key, and R. Mahoney, "Sea and freshwater ice concentration from VIIRS on Suomi NPP and the future JPSS satellites," *Remote Sens.*, vol. 8, no. 6, 2016, Art. no. 523. Doi: 10.3390/rs8060523.

Walter N. Meier received the B.S. degree in aerospace engineering from the University of Michigan, Ann Arbor, MI, USA, in 1991, the M.S. and Ph.D. degrees in aerospace engineering sciences from the University of Colorado, Boulder, CO, USA, in 1992 and 1998, respectively, within the university's interdisciplinary Program in Atmospheric and Oceanic Sciences.

He is currently a Research Scientist with the NASA Goddard Space Flight Center Cryospheric Sciences Lab, Greenbelt, MD, USA. Previously, he has worked as a Research Scientist with the National Snow and Ice Data Center, Boulder, CO, as an Adjunct Assistant Professor with the United States Naval Academy, Annapolis, MD, and as a Visiting Scientist with the United States National Ice Center, Washington, DC.

Dr. Meier is a member of the American Geophysical Union.

J. Scott Stewart received the Ph.D. degree in aerospace engineering sciences from the University of Colorado, Boulder, CO, USA, in 2000.

He currently works as an Independent Contractor with specific interests in scientific programming and data set development and analysis.

Yinghui Liu received the B.S. and M.S. degrees in atmospheric sciences from Peking University, Beijing, China, in 1997 and 2000, respectively, and the Ph.D. degree in atmospheric sciences from the University of Wisconsin at Madison, Madison, WI, USA, in 2006.

He is currently an Assistant Scientist with the Space Science and Engineering Center (SSEC), University of Wisconsin at Madison. He has been working in SSEC since 2006. His current research focuses on developing satellite retrieval algorithm for ice products, and trends in cloud, sea ice properties, surface and atmospheric radiation properties, and the atmosphere–sea ice–ocean interactions in the polar regions.

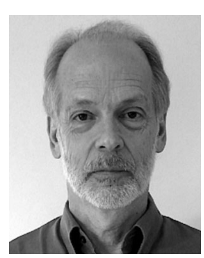

Jeffrey Key received the Ph.D. degree in geography from the University of Colorado, Boulder, CO, USA, in 1988, specializing in satellite meteorology and climatology of the polar regions.

He is the Chief of the Advanced Satellite Products Branch, National Oceanic and Atmospheric Administration's Satellite and Information Service, Madison, WI, USA. Previously, he was an Associate Professor with Boston University.

Dr. Key serves on several international panels and is involved in activities of the World Meteorological Organization and the Group on Earth Observations. He is a member of the American Meteorological Society and the American Geophysical Union.

Jeffrey A. Miller received the B.S. degree from the University of Maryland, College Park, MD, USA, in 1994.

He is currently a Senior Programmer Analyst with ADNET Systems at the NASA Goddard Space Flight Center Cryospheric Sciences Lab, Greenbelt, MD, USA. His work focuses on algorithm development for snow and sea ice data products.